JOURNAL OF MATERIALS SCIENCE 32 (1997) 147–156

On the durability of composite rehabilitation schemes for concrete: use of a peel test

V. M. KARBHARI, M. ENGINEER, D. A. ECKEL II
Department of Applied Mechanics and Engineering Sciences (MC 0085), University of California, San Diego, 9500 Gilman Drive, La Jolla, CA 92093-0085 USA

Composites present a potentially cost-efficient and more durable alternative to the use of externally bonded steel plates for the rehabilitation and strengthening of concrete members, due to their high stiffness-to-weight and strength-to-weight ratios, corrosion resistance and overall ease of application in the field. Although a number of demonstration projects have shown the initial viability of such schemes, a number of critical questions still remain as related to short- and long-term durability as well as damage and failure mechanisms. In this paper a modified peel test is used to investigate the durability of the bond between concrete and composites under five different environmental exposure regimes. Two different epoxies were used with E-glass and carbon fibre reinforced composites. Differences in peel force and interfacial fracture energies based on material and environmental influences are discussed and modes of failure are presented.

1. Introduction

The widespread deterioration of infrastructure due to age, environmental factors and steadily increasing highway traffic patterns (load and frequency) has created a critical need for cost-effective and durable materials and technologies for use in rehabilitation and retrofit. This deterioration of infrastructure elements has lead to a multi-billion dollar problem that is threatening to drastically slow down, if not halt, the progress of our lifelines into the twenty-first century. Of the roughly half million highway bridges in the United States, more than 1100 are either structurally deficient or functionally obsolete due to reasons such as the general age of the structure, steady increase in the weight of highway vehicles (as high as 40% over the design or intended load in some cases [1]) and traffic density, changes in the use of the structure, misdesign, or poor/faulty original construction, deterioration due to environmental attack, and poor maintenance practices. The extensive use of road salt and the effects of severe winters often exacerbates the deterioration, causing spalling of concrete cover and exposure of the steel reinforcement which leads to further accelerated deterioration in addition to a negative psychological effect on commuters as related to safety. The replacement and rebuilding of most of the existing bridge structure, for example, is not a feasible option in most cases for reasons that range from economics (cost of resources) and logistical (excessive disruption of neighbouring facilities, lack of access and new land) to those related to the socio-economic impact of detours/delays/inconvenience over considerably long periods of time on inhabitants, traffic patterns and industrial output. A number of anecdotal cases exist from which a case could be made that delays caused due to detours, traffic jams and slower speeds as a consequence of deteriorated bridges have resulted in industrial losses totaling a significant fraction of national output. Factors such as this make the use of rapid and cost effective strengthening and repair options very attractive. However, the complexity of these efforts is often misunderstood and the project treated as if it were part of routine maintenance. Successful implementation of any strategy for retrofit requires knowledge not only in aspects related to design, but also in material, degradation and durability, and in the analysis of retrofitted structures to predict effects of local response on the entire structural system. This cannot be emphasized sufficiently, since depending on the size, location, complexity and structural state of distress, the cost of rehabilitation can range from $500 000 for a small pedestrian bridge to over $500 000 000 for a large structure such as a major East River crossing [2].

A large number of techniques currently exist for strengthening highway bridges ranging from the use of external post-tensioning to the addition of epoxy bonded steel plates to the tension surface. In 1987, Klaiber *et al.* [3] reported on the use of eight different techniques for the strengthening of existing bridge decks in considerable depth. In 1994 McKenna and Erki [1] reported on the results of a survey aimed at the use of strengthening through external attachment of steel plates. The technique involves the attachment of a steel plate to the tensile surface of the concrete beam, thereby strengthening it through the addition of external reinforcement. Methods of attachment range from adhesive bonding to bolting and combinations thereof. The externally bonded plate increases the flexural stiffness and load-carrying capacity of the

0022–2461

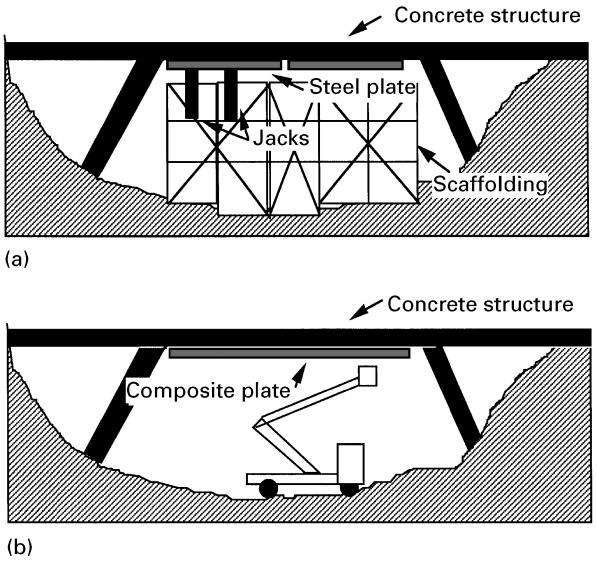

Figure 1 External strengthening through the use of bonded reinforcement plates (a) Steel, (b) Composite.

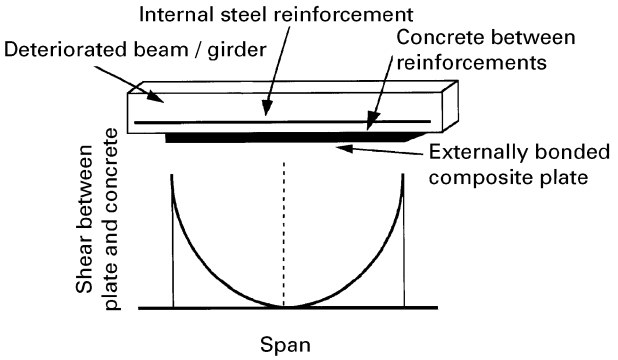

Figure 2 Schematic of hypothetical stress development in a rehabilitated beam showing the development of shear between the plate and concrete.

previously deficient beam, provided the method of attachment enables a reliable transfer of stress between the concrete surface and the plate. Considerable effort has conducted on research to understand this technique [4–10] and engineers have also reported on the results of field implementation ranging from use in apartments to that in arched and prestressed bridge decks [1, 8, 11–15]. Although extensively used in Europe for over a decade, this method suffers from a number of disadvantages ranging from difficulty in placement to concerns related to overall durability. The plates are heavy and, hence, difficult to handle during erection and may be length limited due to weight and size restrictions where utility lines and other obstructions exist. At the minimum jacks, extensive scaffolding and winches or cranes are needed for erection (Fig. 1a). The length restriction necessitates the use of joints which need special attention since on-site welding is not possible due to the destructive effect of heat from welding on the adhesive used between the steel and concrete. In addition to the corrosion that may take place on the steel itself (causing deterioration of the rehabilitation scheme itself!), corrosion at the steel-adhesive/resin interface can be caused by migration of water from the concrete to the interface and steel, which significantly affects the efficiency of the scheme. Studies conducted in 1982 noted that corrosion due to water seepage through concrete and resin towards the steel plate caused a 7–23% reduction in failure loads due to bond distress [16, 17]. There is also the possibility of the bonded steel plate falling off in a buckling mode if loaded in compression such as might happen at or near a cap beam. A major concern, and one that has surprisingly not received significant attention from the community is the danger of corrosion at the steel/epoxy interface which can adversely affect bond durability and response, with premature failure/collapse being the result.

Composite plates, in comparison are lighter and hence easier to handle. They have high specific stiffness and specific strength ratios, outstanding fatigue behaviour and are corrosion resistant. They can conceivably be easily bonded to the concrete surface on site without the use of extensive scaffolding and jacks, requiring a minimal of support equipment (Fig. 1b). In addition to the bonding of a composite laminate to the concrete surface, there is the potential of forming the composite on site using a wet layup technique, thereby allowing its use even in very close quarters and in areas where access is limited. The use of the technique does not necessitate closure of traffic lanes or a major disturbance of existing traffic patterns since extensive scaffolding, barriers, and heavy equipment are not needed. This not only increases the ease of retrofit, but also results in a lower overall systems cost. It must be kept in mind that although the materials cost attributed to composites is higher than that of steel, it is the total systems cost, which includes equipment, time and detour costs, that needs to be considered when making a comparison. Although this technique has been investigated by a number of researchers [18–23] the critical effect of the environment on bond durability and changes in overall response have not been investigated although the deleterious effect of environmental exposure was listed by Neale and Labossière [24], and the importance of testing for effects of environmental exposure prior to field testing was stressed by Saadatmanesh and Ehsani [25].

A major concern with the plating technique irrespective of the plate material, is the debonding or peeling of the plate from the concrete surface. As shown through a hypothetical distribution in Fig. 2, the transition zone at the ends of the plate are subject to sudden changes represented by a region of high shear and low but rapidly changing bending moment which causes high bond stresses on the adhesive/plate and adhesive/concrete interfaces. In the case of thin plates, vertical relative displacement resulting from shear cracks in concrete could also cause the initiation of debonding in regions away from the plate ends (Fig. 3). A number of researchers have noticed debonding and peel during tests on plated beams [7, 8, 20, 26] and have reported concern related to this mode of failure. In general the use of composites, although attractive, makes this mode even more critical due to the anisotropy of the material and the

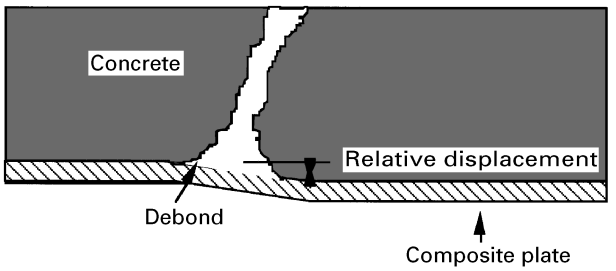

Figure 3 Schematic of failure mode in debonding due to relative movement and interfacial debonding at the concrete-composite interface due to shear.

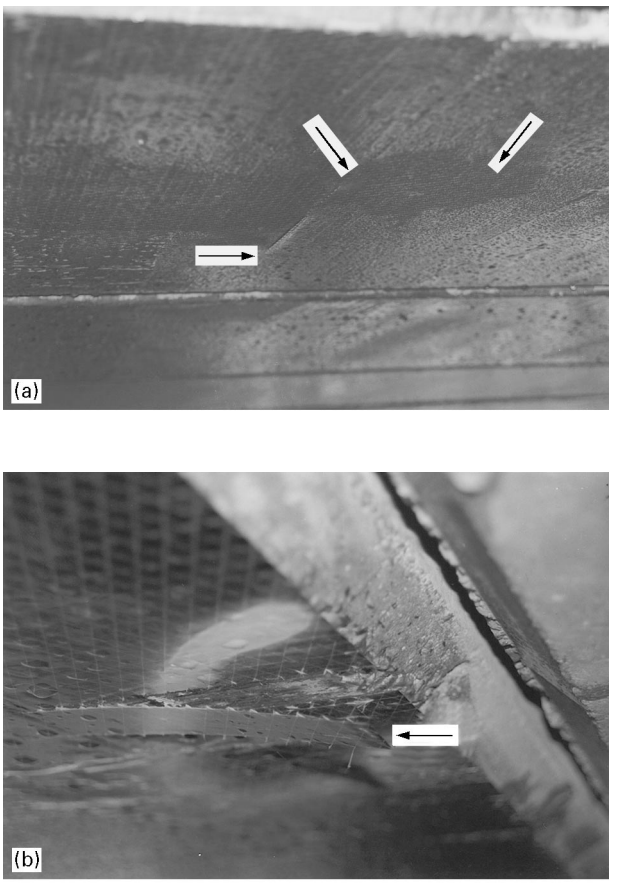

Figure 4 (a) Debonding seen in a rehabilitated structure at an overlap and internally (b) a strip of composite peeled away from an attempted retrofit of a box beam.

sensitivity of most thermosetting resin systems to moisture uptake and plasticization. The concern is further heightened through debonding and peel seen in some existing structures (Fig. 4(a and b) which are of the bottom surface of box beams). Interfacial crack propagation can actually proceed due to a number of reasons including imperfect bonding between the composite and concrete, debonding initiating due to flexural cracking in concrete, peel stresses due to non-uniformities on the concrete surface, fatigue initiated debonding, environmental degradation, incomplete or poor wetout of fibres, and/or the presence of large resin-rich zones. The presence of any of these flaws obviously can lead to further degradation and deterioration including through ease of vandalism at loose edges. Further investigation into the effects of environmental exposure on the viability of the technique and the characteristics of the concrete-composite interface during debonding/peel are thus critical to understanding and evaluating the potential of this technique. The focus of this investigation is on the effects of short-term environmental exposure on the interfacial fracture energies (and, hence, overall durability) through the use of a peel test.

2. Materials and test procedure

Adhesion generally refers to the attraction between two substances, in this case the composite (or resin) and the concrete surface. The attainment of good interfacial contact is obviously a prerequisite for the formation of strong and stable adhesive joints. However, four generic mechanisms of adhesion need to be considered in the investigation of bond, i.e., mechanical interlocking, diffusion theory, electronic theory and absorption theory. In the case of bonding of composites to concrete, the first is by far the dominant mechanism. Mechanical interlocking assumes that the major source of intrinsic adhesion is the interlocking of the resin (in this case) into the irregularities of the concrete surface. The more rough and deep surface topography created through surface abrasion and glass beading creates a structural morphology that allows the resin to penetrate into the irregularities forming a strong interfacial layer. It can be shown that mechanical abrasion not only removes the latence and loose material from the surface to be bonded, but also increases joint strength through the interlocking allowed. Packham [27] has reported on increased adhesion caused by inducing fracture surfaces along tortuous paths caused by irregularities, thereby involving longer lengths (and hence volumes) of the material undergoing plastic type deformation during fracture. The results obtained between concrete and composites are actually more pronounced than those reported by Jennings [28] based on comparisons between bonding to smooth and rough surfaces of aluminium alloys and stainless steel substrates.

The quantification and understanding of bond and peel mechanisms is considered central to the objective of developing a good methodology for the use of externally bonded plates for the rehabilitation and strengthening of deteriorated concrete beams. A number of techniques have been proposed in the past for the measurement of adhesion and interfacial fracture resistance and are listed in references [29, 30] of which the peel mode was considered the most viable since it represents a loading regime and modes of failure that are encountered under service conditions, while providing three distinct advantages over other tests such as the pure shear test, the blister test, etc., i.e.,

(i) bond failure proceeds at a controlled rate
(ii) the peel force is a direct measure of the work of detachment, and
(iii) failure can be achieved under a mixed mode of loading, thereby enabling the evaluation of the critical interfacial fracture energies under both mode I and II loadings (i.e., G_{IC} and G_{IIC}).

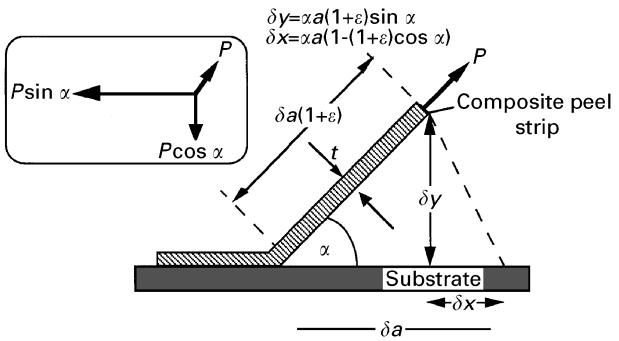

Figure 5 Schematic of the geometrical mechanics of the peel test.

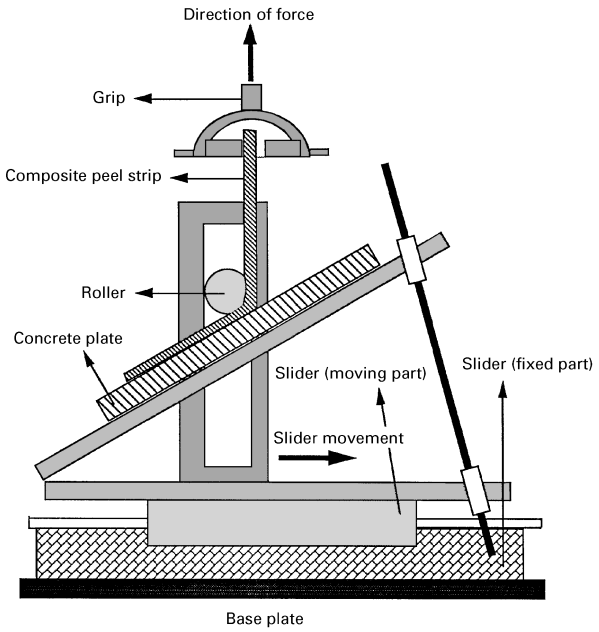

Figure 6 Details of the peel test apparatus.

The peel test procedure described in references [31, 32] was used for the current investigation, wherein actuator movement was recorded using a spring loaded linear variable differential transformer (LVDT). The peel force was directly measured by the load cell and was recorded after appropriate correction for frictional resistance of the slider. A schematic of the mechanics of the test is shown in Fig. 5 and a schematic of the test apparatus is shown in Fig. 6. Further details are reported in references [31, 32]. All tests were conducted at a constant actuator speed of 5.08 mm per min, which meant that the peel rate was determined by the angle of peel used for the specimens.

Concrete blocks of size 22.86 cm (9 in) length, 15.24 cm (6 in) width and 2.54 cm (1 in) depth were cast using 1:3 cement to sand ratio with a water: cement ratio of 0.45, to serve as the substrate. The average 28 day strength and modulus of the concrete was determined to be 25.91 MPa (3757 psi) and 21.53 GPa (3.12×10^6 psi) respectively. The concrete surfaces were abraded to remove latence and to increase the surface area available for bonding, after which the composite was wet-laid up on top of the concrete block using the procedure detailed in reference [33]. The individual peel strips had a length of 30.48 cm (12 in) and width of 2.54 cm (1 in). Each peel strip was made up to two plies of reinforcement (unidirectional fibre sheet, parallel to the length) and was thoroughly wet-out by application of the resin. Care was taken to ensure uniform wet-out and compaction. The composite (as described below) was allowed to cure for 48 h under ambient conditions after which a knife edge was used to ensure clean separation of the peel strips from one another, thereby ensuring that each test was run in an isolated mode.

Both E-glass and carbon reinforcement were used in unidirectional form, with areal weight (weight of dry reinforcement of 300 g m^{-2} each. The carbon fibre sheet had a nominal tensile strength and modulus of 3479 MPa and 227 GPa, respectively, whereas the glass fibre sheet had a nominal tensile strength and modulus of 1515 MPa and 76 GPa, respectively. Both types of reinforcement were held together with a low amount of an epoxy based resin binder ($<5\%$) and glass scrim on one side (placed to increase handleability). The selection of the resin system is very important since it not only serves as the matrix for the composite, but also serves as the adhesive layer between the concrete and the composite itself. Two commercial resin systems were used in this study and will be designated as A and B, the former being similar to that reportedly used for the rehabilitation of adjacent concrete box beams, deterioration of which was shown in Fig. 4(a and b). Both are two component epoxy systems capable of cure at room temperature. The first system was catalysed using a company proprietary hardener using a 2:1 ratio (resin:hardner), whereas the second system was catalysed by Ancamine 1636 in the ratio of four parts resin to one part hardener. System A showed a nominal tensile strength of 46 MPa and a tensile modulus of 3.19 GPa, whereas system B showed values of 60 MPa and 3 GPa for the tensile strength and modulus respectively. Representative tensile properties for the composites tested under ambient conditions are listed in Table 1.

TABLE I Representative composite properties

Resin system	Reinforcement fibre type	Weight fraction (%)	Modulus of elasticity (GPa)	Ultimate tensile strength (MPa)	% strain at failure
A	Glass	57.36	22.68	532.15	2.5
	Carbon	54.82	74.76	1241.67	1.7
B	Glass	55.41	23.43	560.41	2.4
	Carbon	50.79	70.67	1254.32	1.8

After slitting of the peel specimens to ensure that each strip behaved independently, the peel specimens were allowed to cure for one week, after which they were subjected to one of the five different environments for a period of 60 days, namely:

(A): Ambient conditions at 20 °C

(W): Immersion in fresh water at 20 °C

(SW): Immersion in synthetic sea water at 20 °C (ASTM D1141)

(F): Exposure to −15.5 °C

(FT): Freeze–thaw exposure as represented by 24 h alternate cycles of −15.5 °C and +20 °C

The specimens were subjected to controlled peel tests after this exposure.

3. Results and discussion

In analysing any data pertaining to adhesion and peel, data pertaining to the interfacial layer is obviously of great importance. In the case of the structural systems considered in this study, since the composite was formed using wet layup, the resin system intrinsically serves both as the matrix for the composite and the interlayer between the concrete and the composite, i.e., as the adhesive layer. This layer then is the main medium for the transfer of shear stresses between the composite and concrete. Any deterioration of this layer will automatically result in deterioration of the bond between concrete and the external composite plate, thereby causing degradation of the overall rehabilitation strategy. In order to characterize the behaviour of the resin systems, dynamic mechanical analysis (DMA) tests were conducted on neat resin samples (obtained as laid on concrete and cured similar to the peel tests) of both systems . Tests were conducted at room temperature and after immersion in water for one week at 23 °C. Representative DMA plots are shown in Figs 7(a and b) and 8(a and b) for systems A and B, respectively, and overall average results are reported in Table II. The last column in Table II reports the temperature at which the instantaneous modulus (E') tends to the asymptotic value of zero. Values for the glass transition temperature (T_g) were obtained using the peak of the loss modulus curve as the determinator. It is clear that system B has a significantly higher glass transition temperature and is affected to a lesser degree of exposure to water than system A. It should, however, be noted that the rate of decrease of E' from ambient to the point where it is approximately zero is about the same for both resin systems. It is important to note that for rehabilitation schemes, the selection of a resin system with an appropriately high T_g is important since at temperatures higher than the glass transition temperature, the resin becomes deformable and will not be able to transfer shear stresses between the composite and the concrete. There are also serious implications associated with the use of resins or adhesives with glass transition temperatures at or in the low 40's (°C) as related to the threat of fire [34]. Based on results at the resin level it is expected that peel tests would show greater effect of environment exposure on the interfacial fracture energies of

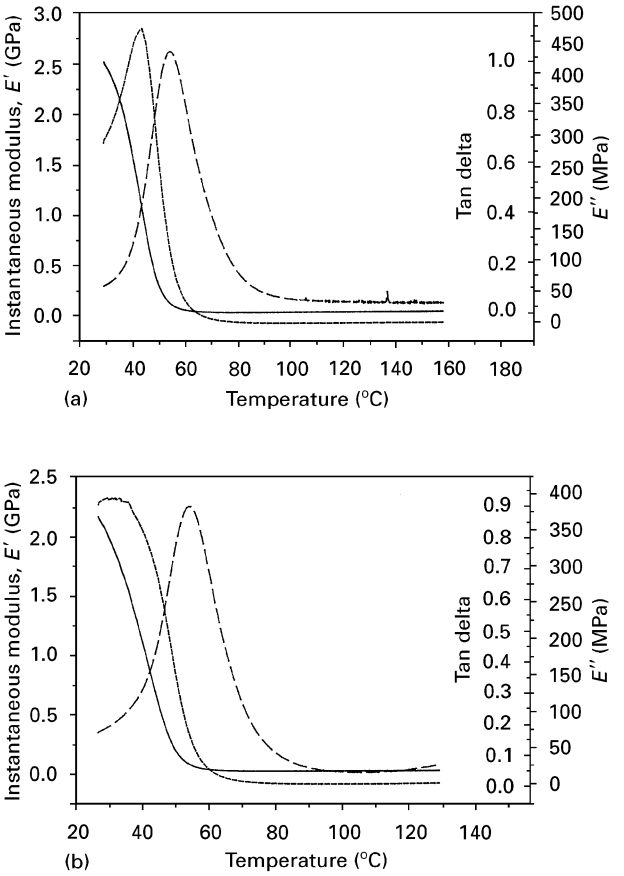

Figure 7 Results of DMA tests on neat resin samples of System A cured on the concrete. DMA tests were conducted after (a) Ambient Exposure (23 °C) and (b) immersion in water for one week at 23 °C Data is shown for; (—) E', (——) Tan δ and (– – –) E''.

systems using resin system A, as will be described in later paragraphs.

Fracture and crack propagation at a bi-material interface (in this case between the resin-composite system and concrete) can generically be characterized by the interfacial fracture energy, G, and the phase angle of loading, Ψ. The phase angle of loading is a measure of the ratio of relative shear to opening experienced by an interface crack and is hence of value in determining the components of mode I and II interfacial energies. Following the approach detailed in reference [35, 36] the phase angle of loading can be expressed as

$$\tan^2 \Psi = \left(\frac{\delta_x}{\delta_y}\right)^2 \quad (1)$$

where δ_x and δ_y are the displacements, depicted in Fig. 5. If the interfacial fracture energy, G, or the stress intensity factor, K, is partitioned into the opening and sliding modes, the phase angle can be written as

$$\Psi = \tan^{-1}\left(\frac{K_{II}}{K_I}\right) \quad (2)$$

following reference [37] or as

$$\tan^2 \Psi = \left(\frac{G_{II}}{G_I}\right) \quad (3)$$

following reference [30] where $\Psi = 0^\circ$ relates to pure mode I conditions and $\Psi = 90^\circ$ corresponds to

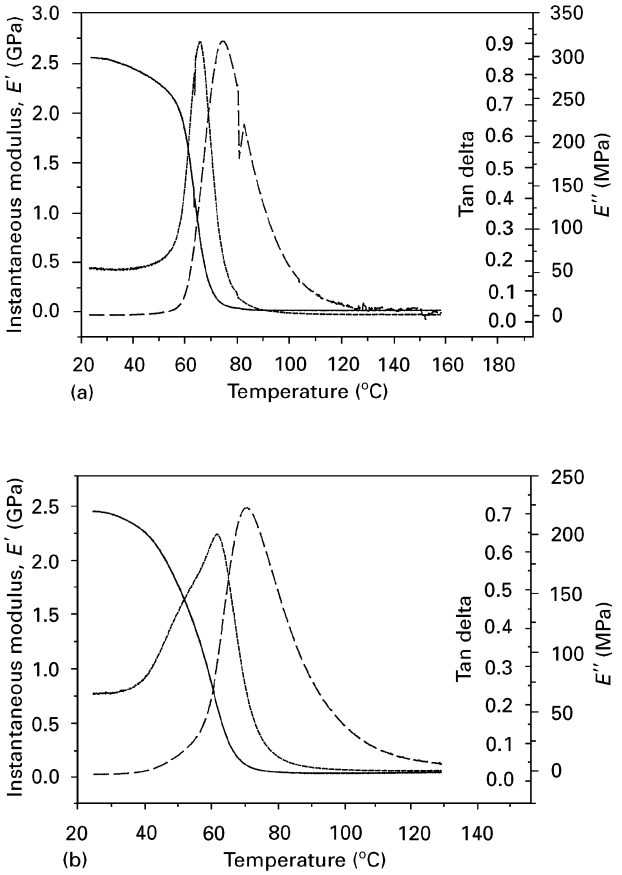

Figure 8 Results of DMA tests on neat resin samples of system B cured on concrete. DMA tests were conducted after (a) Ambient Exposure (23 °C) and (b) immersion in water for one week at 23 °C Data is shown for; (—) E', (— —) Tan δ and (– – –) E''.

a pure mode II scheme. Figs 9–12 depict plots of the interfacial fracture energy as a function of the phase angle of loading for each of the four material systems considered (A-glass, B-glass, A-carbon, B-carbon) under the five regimes of environmental exposure.

In all cases it is seen that the levels of interfacial fracture energies achieved with resin system A (Figs 9 and 11) are significantly higher than those with resin system B. It was also noted that in the glass-fibre reinforced systems there was a clear distinction between the G–Ψ profiles for the specimens exposed to a sub-zero environment (F and FT) and those exposed to the rest, with the former set having higher values of interfacial fracture energy. It is of considerable interest that the distinction was not as apparent in the carbon fibre reinforced peel specimens as seen in Figs 11 and 12, with the first resin system (A) showing almost no change with phase angle when reinforced with carbon fibres.

It should be noted that the use of the total interfacial fracture energy, G, as a discriminator by itself could be misleading, and should be evaluated in conjunction with (a) the force per unit width achieved when maximum load is reached (this is also known as the peel strength), (b) the actual components of the interfacial fracture energy, G_{I} and G_{II}. Irrespective of whether a fracture mechanics approach, or a stress analysis approach is used, the peel force is found to be inversely proportional to the term $(1 - \cos\alpha)$, where α is the peel angle. This necessarily sets up the fact that peel force is a maximum when $\alpha = 0$, and is a minimum at $\alpha = 180^{\circ}$. This trend is consistently seen in all the tests with the value of P decreasing as the peel angle is increased. In this ideal, simplistic case

$$G = P(1 - \cos\alpha) \tag{4}$$

which leads to an inverse relationship between G and P. It should be noted that at low peel angles, G is not a constant, but is dependent on test geometry and may in fact appear to be higher due to an increasing mode II (shear) contribution. Figs 13(a and b) and 14(a and b) show the relationships apparent between the Peel force, interfacial fracture energy, and components of G and the peel angle for the peel test specimens using resin systems A and B respectively under both ambient Figs (13a and 14a) conditions and those of immersion in water Figs (13b and 14b). In all cases P is seen to decrease with peel angle, beginning to approach an asymptotic limit of P at values of the peel angle between 85–100°. As mentioned earlier G increases with peel angle with the rate of increase being higher at higher values of α. It is of considerable interest that the mode I component of interfacial fracture energy decreases almost linearly with peel angle, whereas the sliding (mode II) component increases almost exponentially under ambient conditions for both systems. The effect of exposure to water, not only results in a decrease in levels of peel force and interfacial fracture energy but also results in a significant change in overall trends, in that the changes in G_{I} and G_{II} are almost linear with change in peel angle for both resin systems. This is significant because it not only signifies an effect in overall response due to water, but also indicates a change in mechanisms during peel. It should be noted that in all cases, the total value of G at any point can be expressed as

$$G = G_{\mathrm{I}} + G_{\mathrm{II}} \tag{5}$$

Water absorption is known to cause two effects at the macroscopic level that lead to deterioration of the resin (and of the composite, and the resin-composite

TABLE II Results of DMA tests

Resin system	Environment	Glass transition temperature T_g (°C)	Tan δ	E' (GPa)	Temperature at which $E' = 0$ (°C)
A	Ambient	44	1.02	2.56	71
	Water	36	0.91	2.18	55
B	Ambient	63.5	0.93	2.53	75.5
	Water	62	0.91	2.45	73

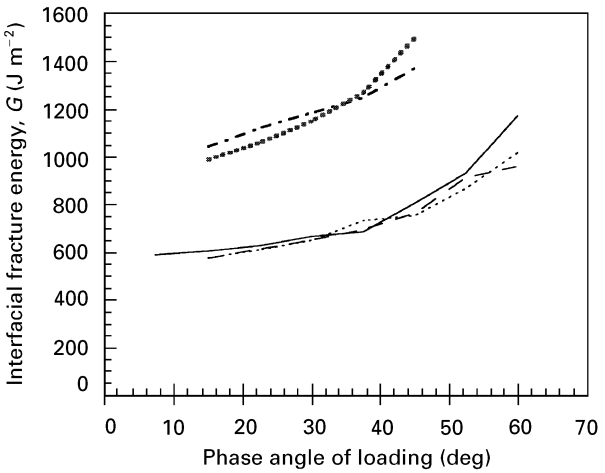

Figure 9 Interfacial fracture energy as a function of phase angle of loading for system A/glass (actuator speed = 5.08 mm per min). Data shown for. (—) A, (— —) w, (– – –) sw, (— · —) F and (■ ■) FT.

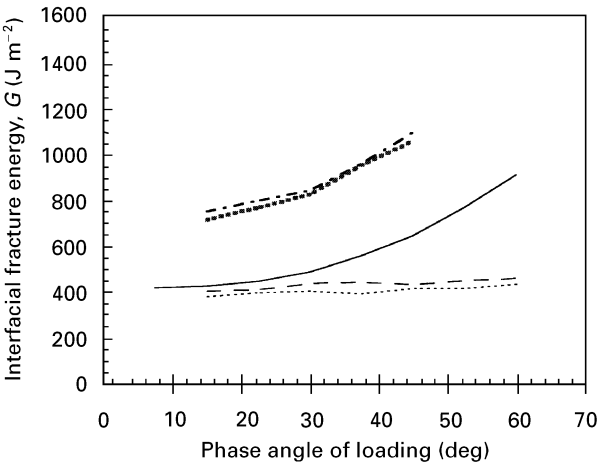

Figure 10 Interfacial fracture energy as a function of phase angle of loading for system B/glass (actuator speed = 5.08 mm per min). Data shown for. (—) A, (— —) w, (– – –) sw, (— · —) F and (■ ■) FT.

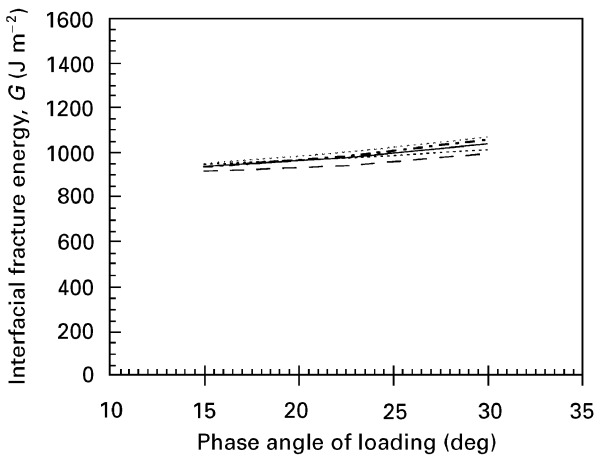

Figure 11 Interfacial fracture energy as a function of phase angle of loading for system A/carbon (actuator speed = 5.08 mm per min). Data shown for. (—) A, (— —) w, (– – –) sw, (— · —) F and (■ ■) FT.

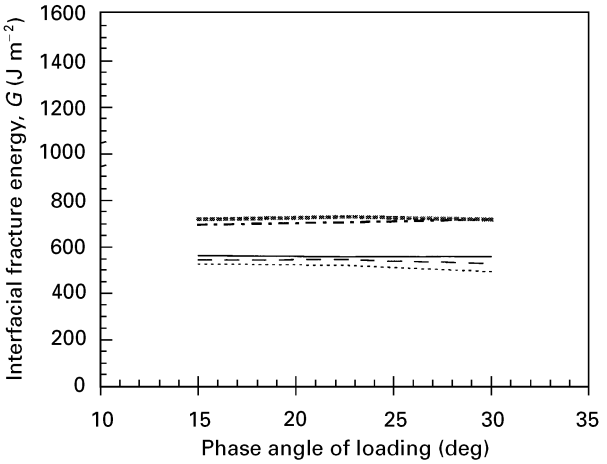

Figure 12 Interfacial fracture energy as a function of phase angle of loading for system B/carbon (actuator speed = 5.08 mm per min). Data shown for. (—) A, (— —) w, (– – –) sw, (— · —) F and (■ ■) FT.

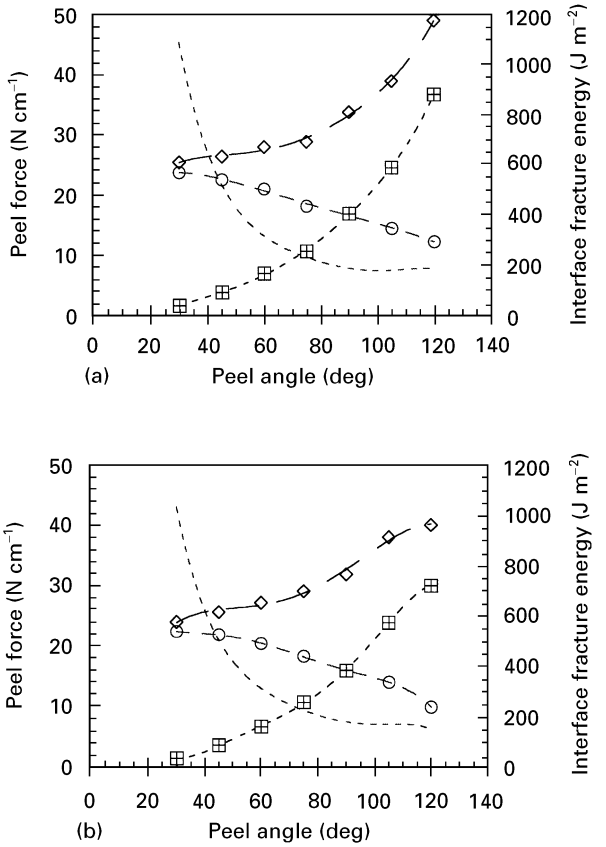

Figure 13 Effect of peel angle on peel force and energies for specimens with resin system A (a) Ambient and (b) Exposed to water. Data shown for. (– – –) P, (◇) G, (○) G_I and (■) G_{II}.

bond), namely a general reduction of performance level, and weight gain due to the uptake of water. Penetration of water into the resin or composite occurs through diffusion and capillary flow through microcracks and voids along imperfect interfaces. Mechanical properties degrade as seen on comparison of Figs 13a and 14a with Figs 13b and 14b respectively, due to plasticization of the resin. In addition debonding stresses across the fibre–resin interface can occur due to resin swelling and osmotic pressure. In

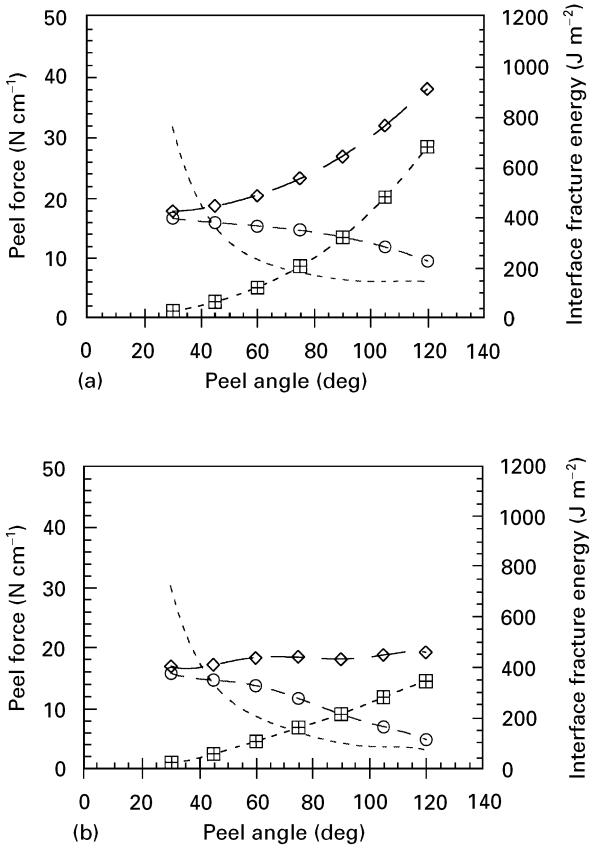

Figure 14 Effect of peel angle on peel force and energies for specimens with resin system B (a) Ambient and (b) Exposed to water. Data shown for. (– – –) P, (◇) G, (○) G_I and (■) G_{II}.

addition it should be noted that the presence of water results in significant degradation of the glass fibre itself. Tests conducted on neat resin samples show that resin system A shows significantly greater water absorption than resin system B. In addition the glass transition temperature also decreased to a greater level in resin system A than for resin system B (see Table II). Although this would intrinsically seem to point to increased degradation in the case of resin system A (as is seen on measurement of load carrying capacity and structural stiffness as in reference [33]), the increased plasticization can lead to misleading levels of toughness at the short term exposure levels.

Although similar trends in terms of increases in G and G_{II} and decreases in P and G_I with peel angle are seen after exposure to a $-15.5\,^{\circ}C$ and a freeze thaw environment, it should be noted that both cause increases in force and interfacial energy levels over those achieved under ambient conditions. At these temperatures stable brittle crack growth is achieved resulting in apparent increases in toughness due to a brittle/ductile transition. The freeze-thaw condition represents a case wherein both localized plasticization and matrix stiffening take place and an exact determination of effects and causes is difficult especially as related to the present case wherein consideration must not only be given to changes in the concrete, composite and the concrete-composite interface, but also due to the effect on increased stiffness on cracking in the peel arm. The interested reader is referred to the works by Dutta [38] and Lord and Dutta [39] for

Figure 15 Micrograph of peel surface under ambient conditions showing intermittent peeling of mortar (Magnification = 18 ×).

a full review of the effects of cold regions type exposures.

It is of interest to compare the behaviour of the glass and carbon fibre reinforced systems within a range of peel angles (30–60°). It was seen that the carbon fibre reinforced systems show greater interfacial fracture energies, although the ratios of mode I to mode II components is approximately the same at each level for the two systems, indicating that the relative amount of opening to shear is largely dependent on the properties of the resin, rather than that of the fibre or composite. In an isotropic material, cracks are generally free to choose a path that maximizes the local energy-release rate. However, an interfacial crack is generally constrained in that it is subject to shear such that the crack-driving force may be greater in a direction other than directly along the interfacial plane. Crack movement away from this plane depends on a number of factors including the relative toughness of the interface and the substrates, the presence of local flaws/defects close to the interfacial plane and the general state of stress in that region. In order to completely understand the mechanisms in the current investigation it is necessary to study both the partitioning of the critical interfacial fracture energy (or toughness) into the opening and sliding modes, as well as to study the morphology existing at the fracture surface. Stereomicroscopy of sample surfaces after peel at increasing values of the peel angle show a distinct movement from a mode I form of fracture (peeling of mortar) to a mixed mode type wherein fracture proceeds along the interface. In addition the effect of exposure to the environment can also cause changes in fracture morphology as can be seen from Figs 15 and 16. Both correspond to the peel surfaces on the concrete side achieved from peel of a specimen of resin system A reinforced with glass and peeled at an angle of 45°. However, Fig. 15 shows the morphology achieved under ambient conditions where peeling of mortar is evident from the rough surface, whereas Fig. 16 depicts the failure almost completely at the resin-composite interface representative of adhesive rather than cohesive failure, due to exposure to water. It should be noted that the carbon fibre systems show the formation of an almost wavy interfacial crack, alternating in the interfacial region between the

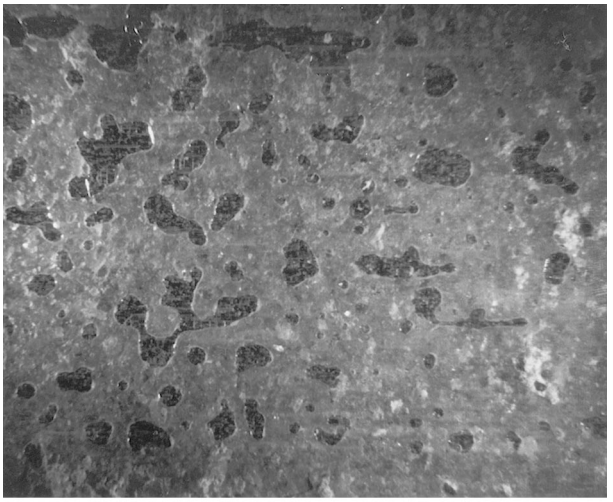

Figure 16 Micrograph of peel surface showing effect of water on peel morphology (magnification = 18 ×).

TABLE III Values of critical energy release rates

Resin/fibre system	Exposure	G_{IC} (J/m^{-2})	G_{IIC} (J/m^{-2})
A-Glass	Ambient (A)	562.54	1656.4
	Water (W)	552.63	1407.4
	Sea-Water (SW)	557.64	1360.0
	−15.5 °C (F)	1025.3	2073.2
	Freeze-Thaw (FT)	940.3	3543.3
B-Glass	Ambient (A)	405.8	1580.1
	Water (W)	408.6	481.2
	Sea-Water (SW)	383.7	447.5
	−15.5 °C (F)	714.1	2328.6
	Freeze-Thaw (FT)	686.4	2454.3
A-Carbon	Ambient (A)	903.9	1902.6
	Water (W)	887.8	1553.7
	Sea-Water (SW)	925.7	1420.1
	−15.5 °C (F)	896.9	2305.0
	Freeze-Thaw (FT)	915.4	2186.8
B-Carbon	Ambient (A)	562.46	558.33
	Water (W)	552.73	485.45
	Sea-Water (SW)	543.04	402.43
	−15.5 °C (F)	689.09	839.64
	Freeze-Thaw (FT)	724.16	723.51

composite and the concrete after exposure to the (F) and (FT) exposures. This may follow the case described by Hutchinson and Suo [40] wherein the interface crack reacts to the presence of flaws in layers adjacent to the two interfaces (concrete and composite) thereby nucleating microcracks. The effect of the mixed mode loading is to push the microcracks back towards the interface resulting in a morphology that depicts a fracture surface covered with "tiny chunks of the layer material" [40].

Extrapolation of material properties, in the form of critical energy levels G_I and G_{II}, is possible by plotting values of the components of the interfacial fracture energy as a function of each other (G_I against G_{II}) and then applying a linear curve fit and obtaining the two intercepts following the procedure detailed in references [31, 41]. Values of G_{IC} and G_{IIC} for the two systems under different environmental exposure conditions are given in Table III. It should be noted that

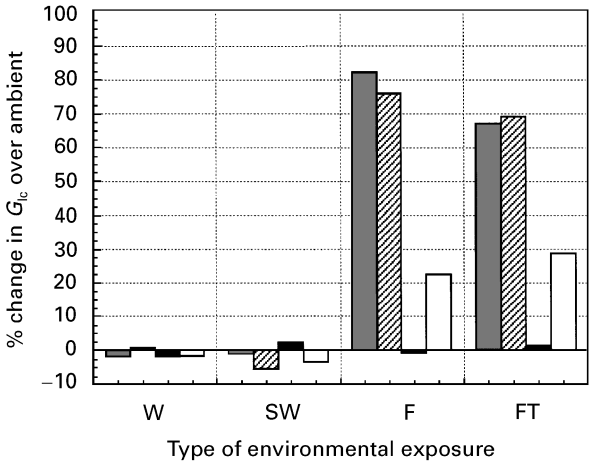

Figure 17 Percentage change in G_{IC} over ambient values as a function of environmental exposure for (▤) A/glass, (▨) B/glass, (■) A/carbon and (□) B/carbon.

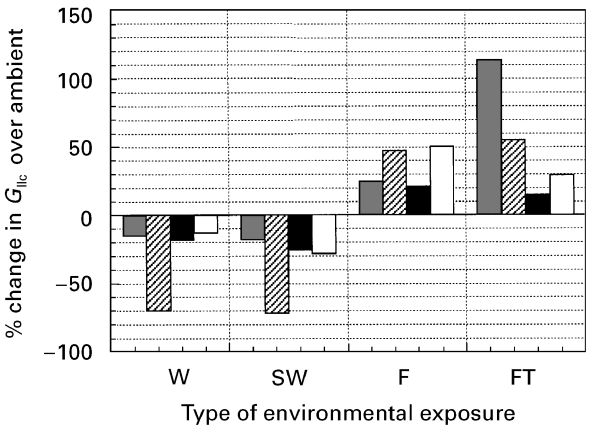

Figure 18 Percentage change in G_{IIC} over ambient values as a function of environmental exposure for (▤) A/glass, (▨) B/glass, (■) A/carbon and (□) B/carbon.

the G_{IC} values are primarily dependent on the properties of the interface, whereas the G_{IIC} values are primarily dependent on the properties of the epoxy. In all cases it can be seen that values achieved with system A are higher than those achieved with system B. Overall, the glass fibre reinforced specimens show a predominance of G_{IIC}, which correlates with an epoxy (i.e., resin) based failure path, due to the susceptibility of glass to deterioration and hence lowering of overall properties of the composite, and the lower stiffness of that system. It is however, perhaps more illuminating to investigate the percentage changes over ambient levels in both systems as a result of environmental exposure, than to study values in isolation. The percentage changes (defined as the ratio

$$\frac{[\text{Exposure values} - \text{Ambient value}]}{\text{Ambient value}} \times 100$$

in G_{IC} and G_{IIC} as a function of environment are shown in Figs 17 and 18 respectively. From Fig. 16 it can be seen that there is very little effect of short-term exposure to water or sea-water on the levels of G_{IC}, although significant levels are seen in G_{IIC} changes in Fig. 17. It is useful to note that although the maximum change in G_{IC} values are achieved after continuous

short-term exposure to the $-15.5\,^{\circ}C$ environment, part of the effect is due to additional stiffening on the peel test itself, rather than completely due to the effect of the environment on the system. Overall, it appears that the carbon fibre based systems shows the least changes. The selection of the resin systems, however, is not as clear since effects vary with fibre and exposure and must also be considered with the results in Table II that suggest a significant lowering of T_g for resin system A. Further investigations of above-ambient temperature and environment, and of resin thickness and type so as to enable the development of a solid base of fundamental knowledge of deterioration science and its role in rehabilitation engineering should be undertaken.

Acknowledgements

The authors gratefully acknowledge the assistance of Drs. Geoff Frohnsdorff and David Ashley of the National Institute of Standards and Technology for assistance with the development of the peel apparatus. Discussions with Professor Roy L. McCullough, Centre for Composite Materials and Department of Chemical Engineering, University of Delaware on the interpretation of physiochemical degradation are also gratefully acknowledged. The assistance of Raghavan Jayaraman and Lei Zhao in characterization is also appreciated. This research was partially funded by ARPA through agreement MDA972-94-3-0030 support of which is gratefully acknowledged.

References

1. J. K. MCKENNA and M. A. ERKI, *Canadian Journal of Civil Engineering*. **21** (1994) 16.
2. New York City Department of Transportation, Bridges and Tunnels (1991), Annual Condition Report.
3. F. W. KLAIBER, K. F. DUNKER, T. J. WIPF and W. W. SANDERS, "Methods of Strengthening Existing Highway Bridges", Transportation Research Board, England, NCHRP Research Report No. 293. (1987).
4. R. JONES and R. N. SWAMY, in Proceedings of the 4th International Congress on Polymers in Concrete, Darmstadt, Germany, pp. 251–255.
5. E. JONES, R. N. SWAMY and A. CHARIF, *The Structural Engineer* **66** (1988) 85.
6. R. N. SWAMY, R. JONES and T. H. ANG, *Int J of Cement Composites and Lightweight Concrete* **41** (1982) 19.
7. R. N. SWAMY, R. JONES and J. W. BLOXHAM, *The Structural Engineer* **65** (1987) 59.
8. R. JONES, R. N. SWAMY, J. BLOXHAM and A. BOUDER-BALAH, *Int J of Cement Composites and Lightweight Concrete* **292** (1980) 91.
9. R. N. SWAMY, R. JONES and A. CHARIF, *The Structural Engineer*, **67** (1989) 45.
10. S. A. HAMOUSH and S. H. AHMED, *ASCE Journal of Structural Engineering* **116** (1990) 356.
11. J. BRESSON, *Annales Publics*, **297** (1972) 2.
12. J. J. DUSSEK, "Strengthening of Bridge Beams and Similar Structures by Means of Epoxy-Resin-Bonded External Reinforcement", Transportation Research Record, 785, Transportation Research Board, England, (1980) pp 21–24.
13. Y. MAEDA, S. MATSUI, I. SHIMADA and H. KATO, "Deterioration and Repairing of Reinforced Concrete Slabs of Highway Bridges in Japan", Osaka University Technology Reports, Vol. 30 [1599], (1980) pp. 135–144.
14. F. ROSTASY and E. RANISCH, in Proceedings of the International Association for Bridge and Structural Engineering: Repair and Rehabilitation of Bridges, Washington, D.C., Vol. 39, pp. 117–122.
15. M. D. MACDONALD and A. J. J. CALDER, *Int J of Adhesion and Adhesives* **2** (1982) 119.
16. A. J. J. CALDER, "Exposure Tests on Externally Reinforced Concrete Beams - First Two Years", Transport and Road Research Laboratory, Crowthorne, England, Report SR529, (1982).
17. G. O. LLOYD and A. J. J. CALDER, "The Microstructure of Epoxy Bonded Steel-to-Concrete Plates", Transport and Road Research Laboratory, Crowthorne, England, Report SR705 (1982).
18. V. MEIER, *Material und Technik* **4** (1987) 125.
19. M. R. EHSANI and H. SAADATMANESH, *Composite Structures* **15** (1990) 343.
20. H. SAADATMANESH and M. R. EHSANI, *ASCE Journal of Structural Engineering* **117** (1991) 3417.
21. T. C. TRIANTAFILLOU and N. DESKOVIC, *ASCE J Engng Mech* **1117** (1991) 1652.
22. P. A. RITCHIE, D. A. THOMAS, L-W. LU and G. M. CONNELLY, *ACI Structural Journal* **88** (1991) 490.
23. U. MEIER, M. DEURING, H. MEIER and G. SCHWEGLER, (1993), in "Alternative Materials for the Reinforcement and Prestressing of Concrete", edited by J. L. Clarke, (Blackie, Glasgow, 1993) pp 153–171.
24. K. W. NEALE and P. LABOSSIÈRE, in Advanced Composite Materials With Applications to Bridges", A. A. Mufti, M. A. Erki and L. G. Jaeger, (Canadian Society for Civil Engineering, Quebec, 1991) pp 21–69.
25. H. SAADATMANESH and M. R. EHSANI, *Concrete International* (1990) 65.
26. V. MEIER and H. KAISER, in "Advanced Composite Materials in Civil Engineering Structures", Proceedings of the ASCE Specialty Conference, (ASCE, New York, NY, 1991) pp 224–232.
27. D. E. PACKHAM, in "Adhesion Aspects of Polymeric Coatings", edited by K. L. Mittal, (Plenum Press, New York, 1983) 19.
28. C. W. JENNINGS, *J of Adhesion* **4** (1972) 25.
29. K. L. MITTAL, *Journal of Adhesion Science and Technology* **1** (1987) 247.
30. A. J. KINLOCH, "Adhesion and Adhesives", (Chapman and Hall, New York, 1987).
31. V. M. KARBHARI and M. ENGINEER, *Journal of Reinforced Plastics and Composites* **15**[**2**] (1996) 208.
32. *idem*, *J Mater Sci Lett*. **14**[**17**] (1995) 1210–13.
33. *idem*, *Journal of Reinforced Plastics & Composites*, (in press).
34. ANON, *Concrete* (1988) 25.
35. J. W. HUTCHINSON, M. E. MEAR and J. R. RICE, *ASME J Appl Mech Trans ASME* **54** (1987) 828.
36. A. G. EVANS, B. J. DALGLEISH, M. HE and J. W. HUTCHINSON, *Acta Metall* **24** (1989) 173.
37. M. D. THOULESS, *Acta Metall et Mater* **40** (1992) 1281.
38. P. K. DUTTA, *ASCE Journal of Cold Regions Engineering* **2** (1988) 124.
39. H. W. LORD and P. K. DUTTA, *Journal of Reinforced Plastics and Composites* **7** (1988) 435.
40. J. W. HUTCHINSON and Z. SUO, in "Advances in Applied Mechanics", Vol. 29, (Academic, 1992).
41. C. C. LAW, A. J. KINLOCH and J. G. WILLIAMS, in the Proceedings of the Adhesion Society, Blacksburg, VA, (1993) pp 96–98.

Received 25 May 1995
and accepted 13 June 1996